# Enhanced two-terminal impedance-based fault location using sequence values

**Muhd Hafizi Idris[1], Mohd Rafi Adzman[1], Hazlie Mokhlis[2], Lilik Jamilatul Awalin[3], Mohammad Faridun Naim Tajuddin[1]**

[1]Faculty of Electrical Engineering Technology, Universiti Malaysia Perlis, Arau, Malaysia
[2]Department of Electrical Engineering, Faculty of Engineering, Universiti Malaya, Kuala Lumpur, Malaysia
[3]School of Advanced Technology and Multidisciplinary, Universitas Airlangga, Surabaya, Indonesia

## Article Info

## ABSTRACT

Fault at transmission line system may lead to major impacts such as power quality problems and cascading failure in the grid system. Thus, it is very important to locate it fast so that suitable solution can be taken to ensure power system stability can be retained. The complexity of the transmission line however makes the fault point identification a challenging task. This paper proposes an enhanced fault detection and location method using positive and negative-sequence values of current and voltage, taken at both local and remote terminals. The fault detection is based on comparison between the total fault current with currents combination during the pre-fault time. While the fault location algorithm was developed using an impedance-based method and the estimated fault location was taken at two cycles after fault detection. Various fault types, fault resistances and fault locations have been tested in order to verify the performance of the proposed method. The developed algorithms have successfully detected all faults within high accuracy. Based on the obtained results, the estimated fault locations are not affected by fault resistance and line charging current. Furthermore, the proposed method able to detect fault location without the needs to know the fault type.

*Corresponding Author:*

Muhd Hafizi Idris
Faculty of Electrical Engineering Technology, Universiti Malaysia Perlis
02600 Arau, Perlis, Malaysia
Email: hafiziidris@unimap.edu.my

## 1. INTRODUCTION

Fault is a phenomenon which can cause the supply of electrical power interrupted. It can happen at any component and location in power system. However, transmission line has the highest probability with fault occurrence because it is exposed to the environment and extreme weather conditions [1]. The causes of fault occurrence are such as lightning strikes, tree and crane encroachment, equipment defect and many other causes [2]. When a fault happened, it must be located fast so that the affected line can be energized back into the network as soon as possible. The longer the time taken for the faulted line to be re-energized, will cause the power system in stress condition and can reduce the power system security and reliability. This happens when other lines becoming overloaded due to the increase of power flow to compensate the power on the faulted line. After a fault occurrence, the maintenance crews will need to check the substation to obtain the fault location information from the installed protection relay. The accuracy of the fault location given by the device is dependent on the algorithm and the measurements it uses. A small error of fault location estimation

can be equivalent to several kilometers at the actual transmission line. Thus, it is difficult task to find the exact fault location.

In the early years, the fault location algorithms were using the measurements at one-terminal only. This is due to most of the relays at that time were standalone type where no communication channel to transfer the data between both connected substations. Examples of one-terminal algorithm which have been used for a long time are such as simple impedance, reactance, Takagi and modified Takagi [3]. One-terminal algorithms still widely used in the present days because the process to replace the electromechanical and static relays will take time and costly. The error produced by the methods which use one-terminal data is significant because many unknown parameters can affect the accuracy of fault location estimation such as fault resistance, remote in-feed current and source impedance [4]. With the advancement of intelligent electronic devices (IEDs) and numerical protection relays, the requirement for the communication between both terminals also increases such as for protection and fault location functions. The devices at both terminals have to be synchronized using a global positioning system (GPS) so that the travelling time delay can be compensated internally in each device [5]. With the availability of measurements from both terminals, fault location algorithms that use data from both terminals will be more accurate. This can be done since many assumptions can be removed to produce accurate fault location. Fault location using two-terminal data basically can be divided into several main methods such as using impedance [6]–[9], travelling wave [10]–[12], neural network [13], [14], optimization [15], and state estimation [16], [17]. The methods also can be classified into using synchronized [9], [18], [19] or unsynchronized [6]–[8], [20] measurements between both terminals.

In impedance-based method, the estimated impedance represents the fault location from the terminal point until the fault point. The recorded data and phasor information were used by Hessine *et al.* [7] to estimate the fault location using apparent impedance calculation. The data from both terminals do not need to be synchronized. Yu *et al.* [6] used the unsynchronized data and estimate the fault location based on reactance calculation. An analytical synchronization of the unsynchronized measurements was performed by Izykowski *et al.* [8]. Then, the fault location was determined using the symmetrical components of the transposed transmission line. The fault location method for line with more than half-wavelength was proposed by Lopes *et al.* [9] where the distributed parameter line model was used instead of a lumped line model. A fault detector based on differential current principle was developed to determine fault occurrence and identify whether the fault is symmetry or not.

The second main method is fault location using travelling wave (TW). The time taken by the waveform to reflect from the fault point is used to estimate the fault location. Lopes *et al.* [10] proposed the TW method which requires neither data synchronization nor line parameter. The time difference between the first incident TW and the successive reflection from the fault point at both terminals were used to estimate the fault location. The first two waves arrival time which recorded inside IED at both ends were used by Naidu and Pradhan [11]. Then, the correct fault location solution was determined using faulted half section identification. The comparison of the rise time for the first TW at both ends was made to determine the faulted section. Andanapalli and Varma [12] used the wavelet transform to capture the travelling time of the transient between fault point and relay location. Then, the fault location was determined using the time difference between the arrival of backward and forward travelling waves. TW methods require very high sampling frequency in the range of MHz for accurate arrival time estimation. Higher sampling frequency will burden the processor and require more memory capacity. Most of the distance relays do not have this very high sampling capability thus the price for the relays which use TW for fault location function definitely higher [5]. An example of relay which uses the travelling wave method is SEL-T401L [21].

Artificial neural network (ANN) has long been used in various applications to solve problems, mainly for a complex data set that has unclear pattern. With no exception, ANN also has been used to estimate the fault location in a power system. Capar and Arsoy [13] used one cycle post-fault voltage and current from one or two-terminal measurements as the training data set. Before training, the measurements were converted to symmetrical components and phasor values using discrete Fourier transform (DFT). ANN method which used both fault and pre-fault voltage and current measurements was proposed Mazon *et al.* [14]. In training period, the method considered both correctly measured magnitudes values and magnitudes affected by errors. The ANN method may produce an error if the actual data used to test the trained system are outside the training data range. Second, the ANN has to be trained with data which consider various parameters and there might exist some parameters which are unknown in reality. Besides that, to train every line in a power network which have different parameters will take a lot of effort and impractical.

Optimization technique is a method used to solve a problem based on the defined objective functions. Huynh *et al.* [15] proposed a method using an improved cuckoo search (ICS) optimization to locate a fault at double circuit transmission line. From the results, the ICS has superior ability compared with cuckoo search (CS), particle swarm optimization (PSO) and genetic algorithm (GA). Genetic algorithm (GA)

was used by Davoudi *et al.* [19] to estimate the fault location. The method was based on distributed time-domain representation and does not require the line parameters. The last method for fault location is using state-estimation by Liu *et al.* [16]. The line was modelled in detail and represented as a multi-section line. Fault location was treated as a state of the dynamic line model and the fault location was estimated using dynamic state estimation algorithm.

Many methods have been researched on estimating the fault location at the transmission line. From the literature, some of the methods did not mention how the fault was detected [6], [8], [13], [14], [16], [19]. Before the fault location can be performed, normal and fault conditions must be differentiated. Once the fault is detected, the fault location process will take place. The fault detection signal can be taken from the relay tripping signal or from the algorithm inside the IED itself. The second important parameter in fault location is charging current. The effect of charging current is very small and can be neglected for a short line. However, the impact of charging current is significant for the long transmission line [22], [23]. This charging current exists during both normal and fault conditions. They are some researchers [7], [8], [16] who used a distributed parameter line model to represent the actual transmission line but no discussion or comparison has been made on the effect of charging current on fault location accuracy.

This paper presents the transmission line fault detection and location using two-terminal measurements. The first algorithm is to detect the fault where the tripping signal from the relay is not required. The fault detection is using the comparison of positive-sequence total fault current between fault condition and pre-fault condition. The second algorithm is the fault location which uses the impedance-based method and negative-sequence values. From the results, the fault location algorithm produced better accuracy using negative-sequence values compared with positive-sequence values due to negative-sequence values have very small effects of charging current. The final fault location was taken at two cycles after the fault detection time. A long transmission line has been modelled using ATPDraw software and the algorithms were developed using MATLAB/Simulink.

## 2. FAULT DETECTION AND LOCATION ALGORITHMS

This section presents the proposed fault detection and location algorithms using the measurements from both local and remote substations. The fault detection and location algorithms are two different algorithms which work together. The function of fault detection algorithm is to detect the fault occurrence at each protected line and differentiate the condition with normal condition. While fault location algorithm is used to estimate the fault location at the faulted line from local terminal. The fault location algorithm will only be initiated once it gets the signal from fault detection algorithm which indicates that a fault just occurred at the protected line.

### 2.1. Fault detection method

The proposed fault detection method uses the comparison of total fault current which flow toward the fault point between pre-fault and fault conditions to decide the fault occurrence. When a fault occurs at a line, both local fault current, $I_{L,F}$ and remote fault current, $I_{R,F}$ will be flowing toward the fault point as shown in Figure 1. Thus, the total fault current, $I_F$ will become very high compared to pre-fault value if both local pre-fault current, $I_{L,PRE}$ and remote pre-fault current, $I_{R,PRE}$ are added together as shown by (1).
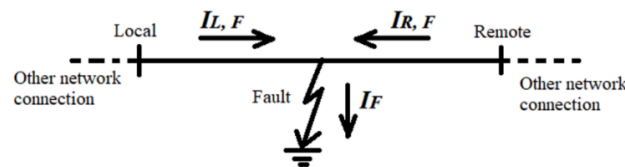


Figure 1. Current flow during fault condition

$$I_F \gg (I_{L,PRE} + I_{R,PRE}) \tag{1}$$

$$I_F = (I_{L,F} + I_{R,F}) \tag{2}$$

The algorithm proposed only uses the positive-sequence values which can be converted directly from the phase values. Thus, the computation is easier compared with the algorithms which computed using the phase values. The positive-sequence versions for total fault current comparison are shown by (3). A fault

at the line will be detected once the total positive-sequence fault current, $I_F^1$ (summation of local positive-sequence fault current, $I_{L,F}^1$ and remote positive-sequence fault current, $I_{R,F}^1$) more than the summation of local positive-sequence pre-fault current, $I_{L,PRE}^1$ and remote positive-sequence pre-fault current, $I_{R,PRE}^1$.

$$I_F^1 \gg (I_{L,PRE}^1 + I_{R,PRE}^1) \tag{3}$$

$$I_F^1 = (I_{L,F}^1 + I_{R,F}^1) \tag{4}$$

A threshold can be set to determine the fault condition as shown in (5).

$$I_F^1 > n \ x \ (I_{L,PRE}^1 + I_{R,PRE}^1) \tag{5}$$

where, $n > 1$ (constant).

During normal condition, there will be no difference between $I_F^1$ and the summation of $I_{L,PRE}^1$ and $I_{R,PRE}^1$ as shown by (6). The situation for normal condition is shown in Figure 2 where the currents from both terminals will always be in the same direction where one will be exporting the power and the other one will be importing the power.
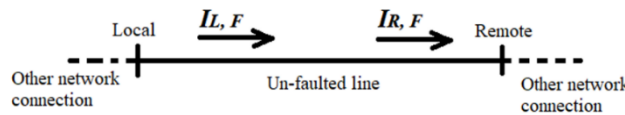


Figure 2. Current flow during normal condition

$$I_F^1 = (I_{L,PRE}^1 + I_{R,PRE}^1) \tag{6}$$

At normal condition, theoretically, the value of $I_F^1$ will be zero because of both positive-sequence pre-fault currents, $I_{L,PRE}^1$ and $I_{R,PRE}^1$ are in the same direction. However, $I_F^1$ has a small value due to the effect of line inductance and capacitance. To differentiate between normal and fault conditions, the threshold, $n$ can be set more than one where the present value of $I_F^1$ will be compared with the multiplication of $n$ with previous one cycle value (pre-fault value) of $I_F^1$ (refer (5)). At fault condition, the current from both terminals will be flowing toward the fault point (opposite direction) which will result in a very high value of $I_F^1$. Thus, this very high value of $I_F^1$ can be easily detected using the threshold setting, $n$ which is slightly more than one. The reason why negative-sequence values were not chosen for the comparison of the total fault current between fault and pre-fault conditions is that during pre-fault time, all phases are in balance condition, thus the negative-sequence values are very small, and this will make it difficult to make the comparison with the values during fault condition.

## 2.2. Fault location method

The fault location algorithm proposed in this research was developed based on two-terminal fault location method [5]. This method requires measurements from both terminals. The measurements from both terminals are assumed to be synchronized. Figure 3 shows a transmission line with a fault at a point between local and remote terminals.
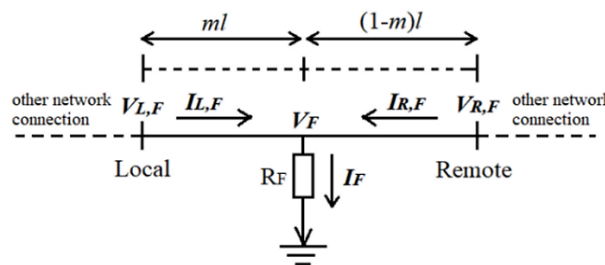


Figure 3. A transmission line with a fault between local and remote terminals

As can be seen from Figure 3, a fault occurred at *ml* kilometer from local substation and *(1-m)l* kilometer from remote substation where *m* is fault location in per unit and *l* is the line length in kilometer. The voltage at the fault point, $U_F$ has equal values when measured from both ends. The currents from both terminals will flow toward the fault point and through the fault resistance, R$_F$ which is unknown. The summation of these two currents equal to the total fault current, $I_F$. The voltage equations as seen from local and remote terminals are shown by (7) and (8) respectively.

$$U_L = mlZ_{L-R}I_L + U_F \tag{7}$$

$$U_R = (1-m)lZ_{L-R}I_R + U_F \tag{8}$$

where the line impedance per km,

$$Z_{L-R} = R_{L-R} + jX_{L-R} \tag{9}$$

$R_{L-R}$   : line resistance per km
$X_{L-R}$   : line reactance per km
$I_L$       : line current measured from local terminal
$I_R$       : line current measured from remote terminal

By arranging both (7) and (8) for $U_F$, it will obtain (10) and (11).

$$U_F = U_L - mlZ_{L-R}I_L \tag{10}$$

$$U_F = U_R - (1-m)lZ_{L-R}I_R \tag{11}$$

Then, both (10) and (11) were equalized as in e (12) until (14).

$$U_L - mlZ_{L-R}I_L = U_R - (1-m)lZ_{L-R}I_R \tag{12}$$

$$U_L - mlZ_{L-R}I_L = U_R - lZ_{L-R}I_R + mlZ_{L-R}I_R \tag{13}$$

$$U_L - U_R + lZ_{L-R}I_R = mlZ_{L-R}(I_L + I_R) \tag{14}$$

Based on e (14), it was arranged for *m* and will obtain,

$$m = \frac{U_L - U_R + lZ_{L-R}I_R}{lZ_{L-R}(I_L + I_R)} \tag{15}$$

As shown in (15) for *m* which is in per unit can be separated into three different forms based on sequence components which are positive, negative and zero-sequences as shown by (16), (17) and (18) respectively. Both $Z_{L-R}^1$ and $Z_{L-R}^0$ can be calculated based on (9) using each sequence parameters for the line. Line negative-sequence impedance, $Z_{L-R}^2$ is equal to $Z_{L-R}^1$. To get the fault location in kilometer, *m* has to be multiplied with the line length. The fault location can be calculated using these three *m* sequence equations. The zero-sequence component only exists during ground faults thus the zero-sequence equation for *m* is not suitable to be used to estimate fault location for unground faults where the zero-sequence component is not existing. The positive-sequence component exists in all types of faults including both symmetrical and unsymmetrical faults while the negative-sequence component will only exist during unsymmetrical faults. This research proposes a fault location method using a negative-sequence (17) because it is less affected by line charging current compared with the algorithm using a positive-sequence equation. Theoretically, the negative-sequence component cannot be used to estimate the fault location for symmetrical three-phase fault. However, this is not a problem. In a practical fault condition, it is impossible for symmetrical three-phase fault which has the same values of fault impedance between phases to happen. There must be at least a slight difference in fault impedance between different phases. Although a three-phase fault has a very slight difference of fault impedance between phases, the negative-sequence component will exist due to small imbalance conditions. Thus, the negative-sequence equation can be used to estimate the fault location for three-phase fault.

$$m = \frac{U_L^1 - U_R^1 + lZ_{L-R}^1 I_R^1}{lZ_{L-R}^1 (I_L^1 + I_R^1)} \tag{16}$$

$$m = \frac{U_L^2 - U_R^2 + lZ_{L-R}^2 I_R^2}{lZ_{L-R}^2 (I_L^2 + I_R^2)} \tag{17}$$

$$m = \frac{U_L^0 - U_R^0 + lZ_{L-R}^0 I_R^0}{lZ_{L-R}^0 (I_L^0 + I_R^0)} \tag{18}$$

To measure the performance of fault location algorithm, (19) was used to compare between actual, $FL_{actual}$ and estimated, $FL_{estimated}$ fault locations.

$$\% \text{ Error} = \frac{FL_{estimated}\ (km) - FL_{actual}(km)}{\text{Line Length (km)}} \times 100 \tag{19}$$

## 3.   COMBINATION OF FAULT DETECTION AND LOCATION METHODS

The flowcharts for fault detection and location methods are shown in Figures 4 and 5 respectively. For fault detection, firstly, both local and remote three-phase currents will be continuously measured by the fault detector. Then, the current measurements for both ends will be converted to their equivalent positive-sequence values. The positive-sequence values of currents from both ends will be added together to get the total positive-sequence current. Next, this current will be hold one cycle to represent the pre-fault value. After that, the present value of total current will be compared with the threshold current setting (*n* times pre-fault total current value). If the present total current is more than the threshold current, the fault is detected, and a signal will be sent to fault location algorithm to estimate the distance of fault point from local end. The fault detection scheme will continue to measure the currents and the flow is repeated when no fault been detected.
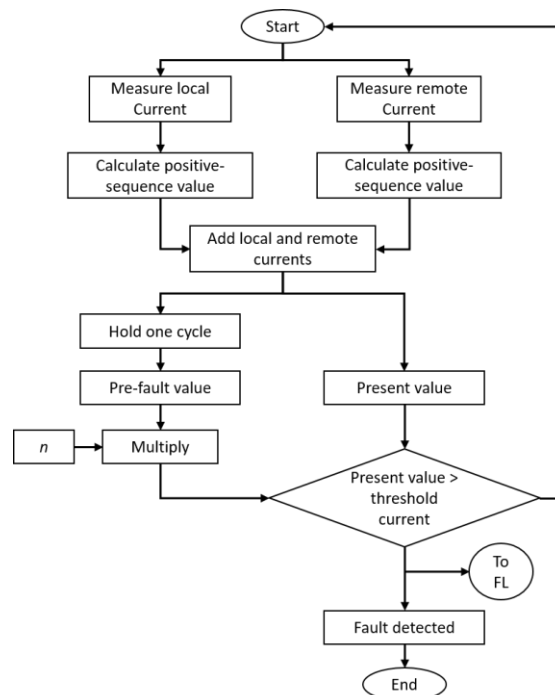


Figure 4. Flowchart of fault detection method

Next, for fault location in Figure 5, the fault locator will continuously measure the current and voltage from both ends of the line. Then, the negative-sequence values for both end measurements will be calculated. Using negative-sequence values, the fault location will be estimated continuously based on (17) no matter what the line condition is. When the fault locator gets a signal from fault detector (FD=1) indicating that a fault just occurred at the line, the fault locator will take the estimated fault location at two cycles starting from fault detection time. Finally, the fault location from local terminal will be displayed. When no signal been received by the fault locator (FD=0) from fault detector, the overall process of fault location is repeated but no-fault location estimation been taken.
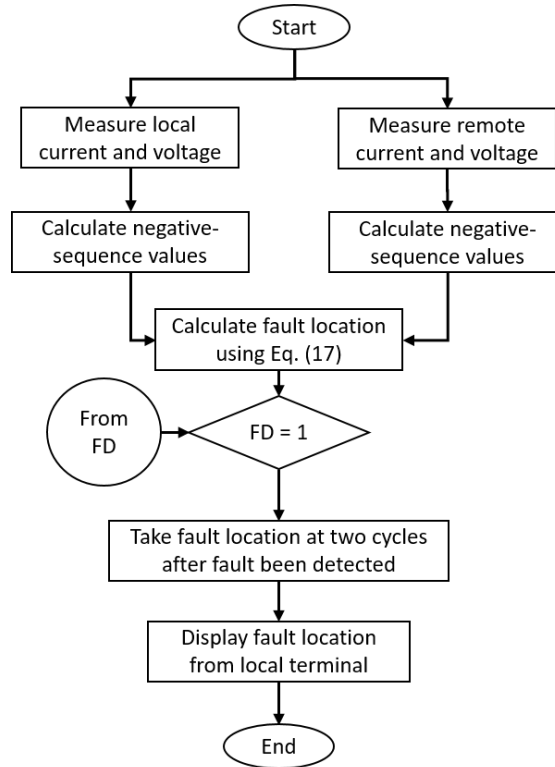
Figure 5. Flowchart of fault location method

## 4.   METHOD

This section presents the development of fault detection and fault location algorithms on transmission line. The two-terminal transmission line has been modelled using ATPDraw software. The network connections at the back of local and remote substations were presented by the equivalent voltage sources. The type of the line used was distributed parameter line where the resistor, inductor, and capacitor (RLC) parameters are distributed uniformly along the line. The long transmission line has been chosen in this work due to the total charging current is very high. The parameters for the transmission line are listed below. The line parameters are taken from line 1-to-2 in 39-bus New England network [24].

- Line length=275.5 km
- Rated voltage=500 kV
- Nominal frequency=60 Hz
- Positive-sequence resistance=0.032 Ω/km
- Positive-sequence inductance=0.989413 mH/km
- Positive-sequence capacitance=0.002692 µF/km
- Zero-sequence resistance=0.318 Ω/km
- Zero-sequence inductance=2.968240 mH/km
- Zero-sequence capacitance=0.001615423 µF/km

Different fault locations, fault types and fault resistances have been simulated using the line model in ATPDraw and the measurements for all fault conditions were transferred to MATLAB/Simulink software where the fault detection and fault location algorithms were developed. The developed algorithms of fault detection and location were combined and shown in Figure 6. There are five main subsystems, namely two-terminal measurements, positive-sequence conversion, negative-sequence conversion, fault detection algorithm and fault location algorithm subsystems.

The blocks inside fault detection algorithm subsystem are shown in Figure 7. This subsystem is used to detect the fault occurrence at the protected line and send a signal to fault location subsystem. As can be seen in the figure, the combination value of local, $I_L^1$ and remote, $I_R^1$ positive-sequence currents will always be compared between present time and previous one cycle time. Thus, when a fault happened, the combination of these two currents will be very high compared with their combination value for the previous one cycle which is during pre-fault. The transport delay block (dashed circle) is used to delay the combination value of both currents to represent the pre-fault value. The D-latch block is used to maintain the detection signal while

the delay 2 cycles block is used to stop the simulation at 2 cycles after a fault has been detected. Hence, the fault location value at the simulation stop time will be taken as the final fault location value.
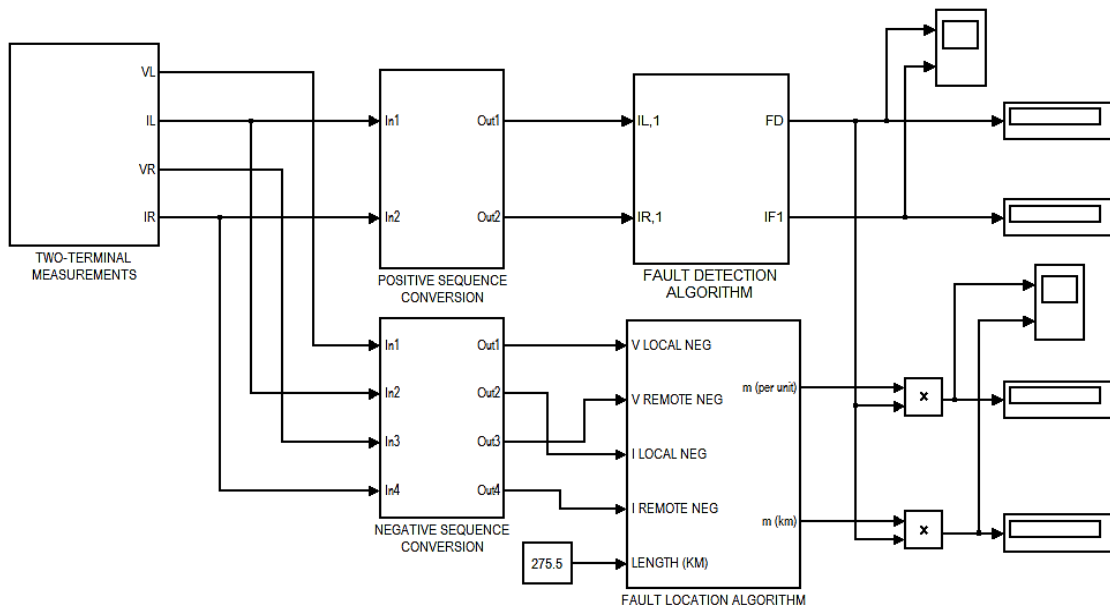


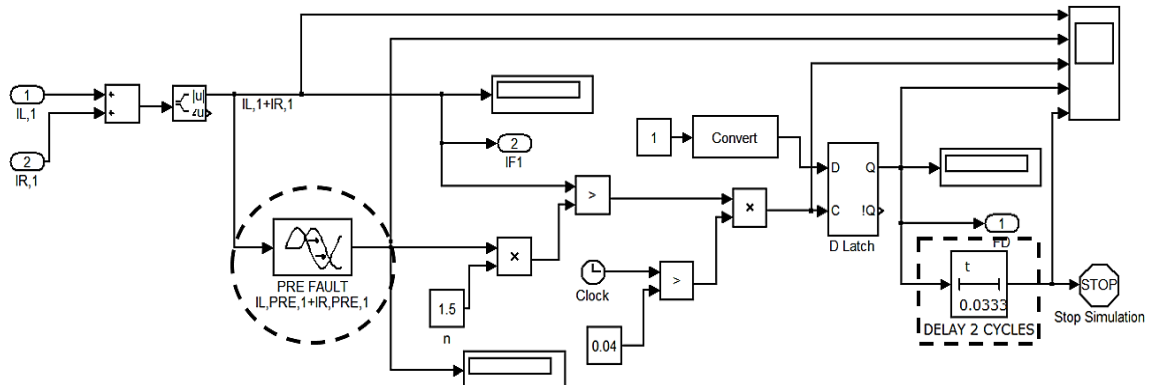Figure 6. Combined fault detection and location algorithms developed using MATLAB/Simulink



Figure 7. Blocks inside fault detection algorithm subsystem

A threshold value of 1.5 times the pre-fault value was set to detect the fault. When the current combination value is more than this threshold setting, fault is detected. This constant 1.5 is sufficient since the pre-fault combination value is very small because both currents at that time are in the same direction. When a fault occurred, both currents will be in opposite direction thus the value will be very high and far from threshold current setting. After a fault is detected, the fault location estimation will be taken at two cycles starting from the edge of fault detection. This was realized using the on/off delay block (dashed box) where the simulation will be stopped after the delay finished. The last value of the estimated fault location at the stop time will be taken as the final fault location.

Figure 8 shows the blocks inside fault location algorithm subsystem. The blocks were arranged based on (17). The outputs from this subsystem are the fault location, $m$ in per unit and in kilometer. The line impedance was calculated inside compute $Z_1$ subsystem and the blocks inside this subsystem are shown in Figure 9. The subsystem in Figure 9 uses the positive-sequence parameters to calculate the negative-sequence line impedance-based on (9). The parameters required are per km values of positive-sequence line resistance ($R_1$) and inductance ($L_1$), nominal frequency ($f$) and line length ($l$).
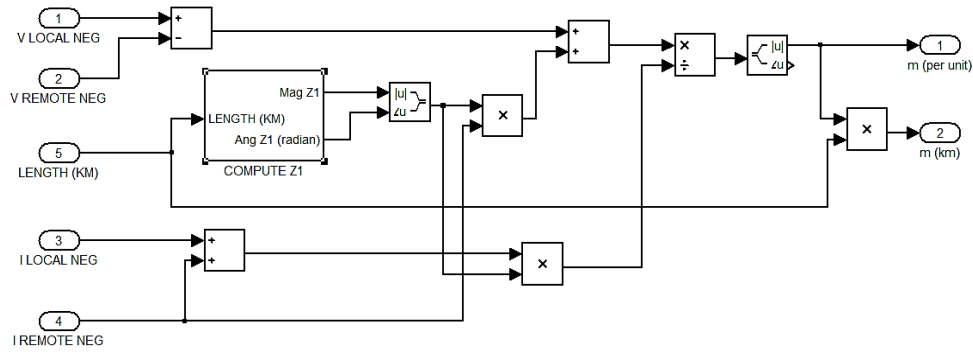
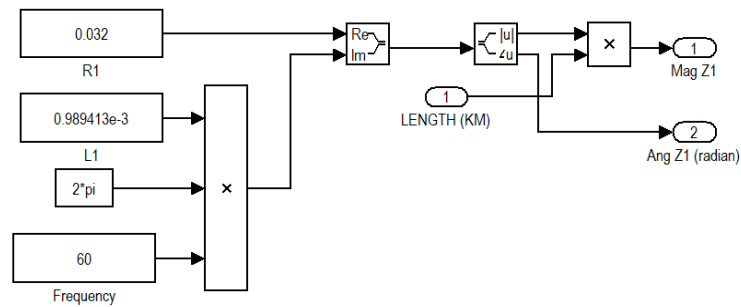Figure 8. Blocks inside fault location algorithm subsystem



Figure 9. Blocks inside compute $Z_1$ subsystem

## 5.   RESULTS AND DISCUSSION

This section presents the results of fault detection and fault location algorithms. As been mentioned earlier, the fault detection algorithm uses the positive-sequence values while the fault location algorithm uses the negative-sequence values. First, an example is shown on how the proposed method detected and located a single line-to-ground fault. Then, followed by the test on the effect of fault resistance, test for various fault conditions, comparison between positive and negative sequence values as the inputs to fault location and finally, the test on three-phase fault using negative sequence values.

### 5.1.  An example of fault detection and location operation

To show the example of the waveform and how the method works, a red phase-to-ground fault was simulated from 0.1 to 0.15 s, at 20% (55.1 km) from the local terminal with 15 Ω of fault resistance. Figures 10(a) and 10(b) show the phase currents measured from local and remote terminals respectively. It can be seen that the red phase current increased significantly after 0.1 s for both terminals. The maximum red phase current for the local terminal (9,534 A) is higher than the maximum red phase current for the remote terminal (2,466 A). This is because the fault occurred at a point nearer to the local terminal (20% from the local terminal) than the remote terminal.
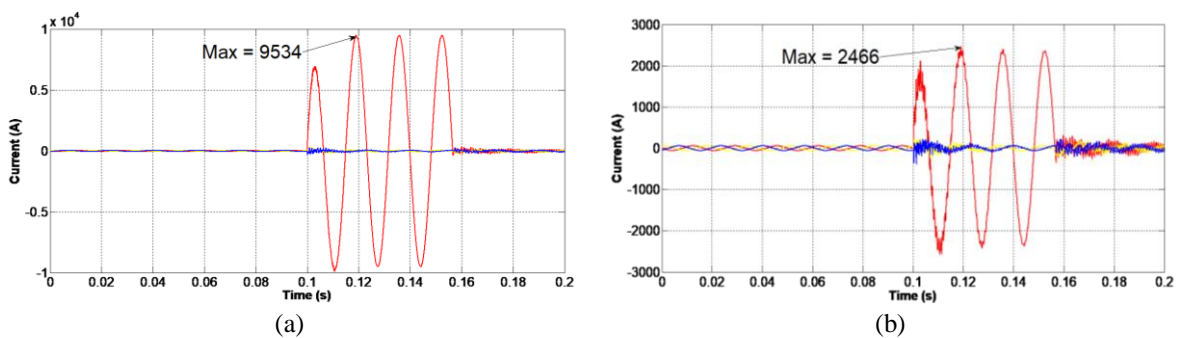


(a)



(b)

Figure 10. Measured phase currents for; (a) local terminal and (b) remote terminal

*Enhanced two-terminal impedance-based fault location using sequence values (Muhd Hafizi Idris)*

Figure 11 shows the results combination of Figure 11(a) total local and remote currents summation, Figure 11(b) total current which has been hold and delayed for one cycle, Figure 11(c) fault detection signal and Figure 11(d) simulation stop signal. At 0.102 s (0.002 s time difference from fault initiation), the fault was detected after the total current (222.3 A) more than the threshold current setting which was equal to 172.2 A (1.5 times the pre-fault total current of 114.8 A at 0.102 s). At 0.1353 s (approximately two cycles after fault detection time), the simulation was stopped where the estimated fault location was taken as the final value. Figure 12 shows the final fault location value equal to 55.13 km with an error of 0.03 km or 0.01089%.
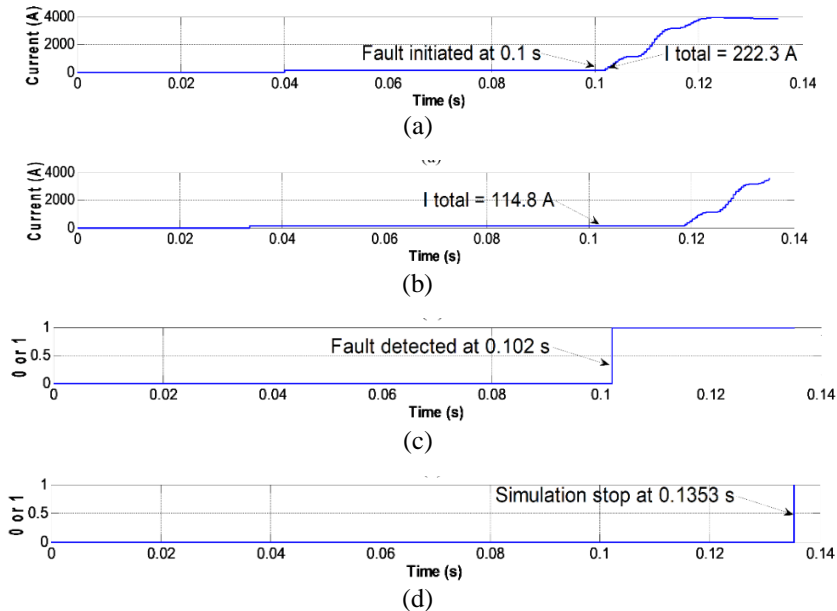


Figure 11. Results combination of fault detection for red phase-to-ground fault (a) total local and remote currents summation, (b) total current which has been hold and delayed for one cycle, (c) fault detection signal, and (d) simulation stop signal
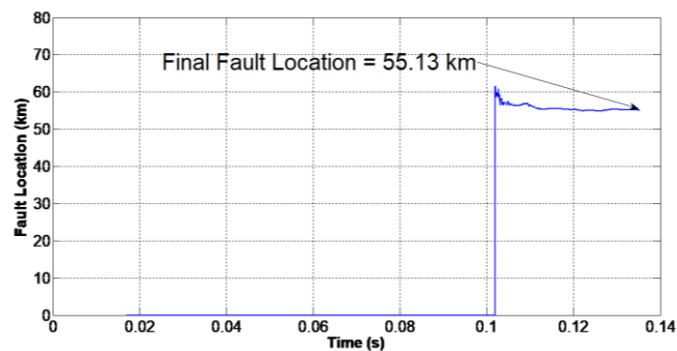


Figure 12. Final fault location at two cycles after fault detected

## 5.2. The effects of fault resistance on fault location accuracy

Three different types of faults have been simulated and tested to compare the accuracy of fault location estimation for different fault resistance values. Figures 13 to 15 show the results of fault location errors for single line-to-ground fault (SLG), line-to-line (LL) fault and double line-to-ground (LLG) fault respectively. For each fault type, the fault resistance was varied for 0.1, 20 and 50 Ω. For each fault resistance, the fault location also was varied from 10% until 90% of the line length from the local terminal with a 10% step. From all those three figures, it can be seen that there is no significant difference in fault location error between different fault resistance values. This shows that the fault resistance has no effect on the proposed fault location algorithm. All the errors are near zero and no error more than 1%.
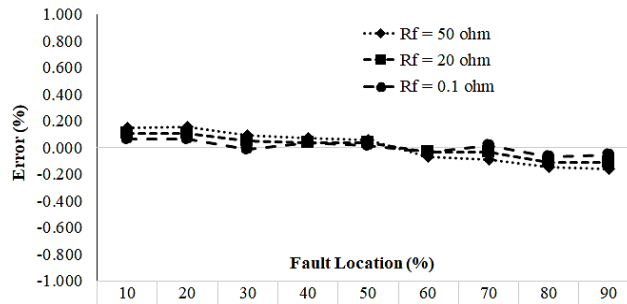
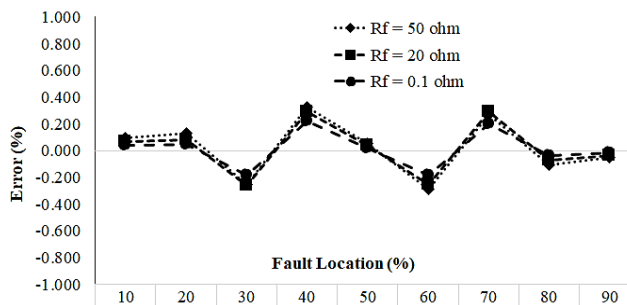Figure 13. SLG fault with different fault resistances and fault locations



Figure 14. LL fault with different fault resistances and fault locations
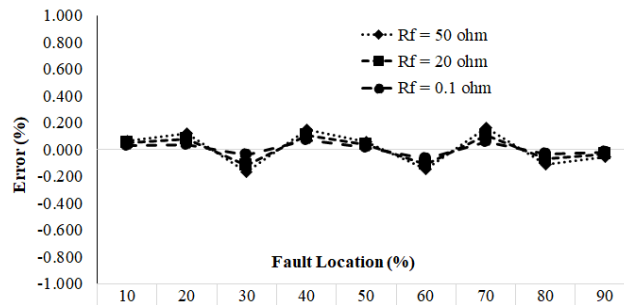


Figure 15. LLG fault with different fault resistances and fault locations

The reason why fault resistance does not affect fault location accuracy is because by using two-terminal data from both local and remote terminals, the value of fault resistance is not required in two-terminal algorithm. This is not true for fault location algorithms which only use one-terminal data where fault resistance is unknown and normally been estimated using many assumptions or left unknown thus can greatly affect the fault location accuracy if the actual fault resistance is very high.

## 5.3.  Fault detection and fault location for various fault conditions

As been mentioned earlier, the fault detection algorithm uses the positive-sequence values to detect the fault while the fault location algorithm uses the negative-sequence values. Three types of unsymmetrical faults with different fault resistances and fault locations have been simulated and the results of fault detection and location are shown in Table 1. All faults were initiated at 0.1 s. As can be seen from Table 1, all faults have been successfully detected and located. When the faults occurred, the combination value between positive-sequence local current and remote current were very high compared with their combination value during pre-fault time. It was possible due to during fault time, both currents were in opposite direction. Thus, the fault occurrences were easily detected. From the results, the average fault detection time is 0.1018 s and the average time period between fault detection time and fault initiation time is 0.0018 s which is about 0.108 cycle. This shows that the fault detection algorithm is very fast in detecting any fault occurrence even for very high fault resistance. The results of the estimated fault location as in Table 1 were taken at two

cycles after fault detection time. The average error of fault location produced for various fault conditions is 0.0678 km and the average error in percentage is 0.0246%. The results of fault location estimation are very accurate where there is no estimated fault location which more than 1 km or more than 1% thus the algorithm is reliable.

Table 1. Results of fault detection and location algorithms for three different fault types

| No | Fault Type | $R_F$ (Ω) | Actual Fault Location (%) | Actual Fault Location (km) | Fault Detected (Yes/No) | Fault Detection Time (s) | Fault Detection Time-Fault Initiation Time (s) | Estimated Fault Location (km) | \|Error (km)\| | \|Error (%)\| |
|---|---|---|---|---|---|---|---|---|---|---|
| 1 | SLG | 0.1 | 10 | 27.55 | YES | 0.1015 | 0.0015 | 27.620 | 0.070 | 0.025 |
| 2 | | | 50 | 137.75 | YES | 0.1020 | 0.0020 | 137.800 | 0.050 | 0.018 |
| 3 | | | 90 | 247.95 | YES | 0.1015 | 0.0015 | 247.900 | 0.050 | 0.018 |
| 4 | | 20 | 10 | 27.55 | YES | 0.1015 | 0.0015 | 27.630 | 0.080 | 0.029 |
| 5 | | | 50 | 137.75 | YES | 0.1025 | 0.0025 | 137.800 | 0.050 | 0.018 |
| 6 | | | 90 | 247.95 | YES | 0.1015 | 0.0015 | 247.900 | 0.050 | 0.018 |
| 7 | | 50 | 10 | 27.55 | YES | 0.1020 | 0.0020 | 27.640 | 0.090 | 0.033 |
| 8 | | | 50 | 137.75 | YES | 0.1025 | 0.0025 | 137.800 | 0.050 | 0.018 |
| 9 | | | 90 | 247.95 | YES | 0.1020 | 0.0020 | 247.900 | 0.050 | 0.018 |
| 10 | LL | 0.1 | 10 | 27.55 | YES | 0.1015 | 0.0015 | 27.660 | 0.110 | 0.040 |
| 11 | | | 50 | 137.75 | YES | 0.1020 | 0.0020 | 137.800 | 0.050 | 0.018 |
| 12 | | | 90 | 247.95 | YES | 0.1015 | 0.0015 | 247.800 | 0.150 | 0.054 |
| 13 | | 20 | 10 | 27.55 | YES | 0.1015 | 0.0015 | 27.620 | 0.070 | 0.025 |
| 14 | | | 50 | 137.75 | YES | 0.1020 | 0.0020 | 137.800 | 0.050 | 0.018 |
| 15 | | | 90 | 247.95 | YES | 0.1015 | 0.0015 | 247.900 | 0.050 | 0.018 |
| 16 | | 50 | 10 | 27.55 | YES | 0.1015 | 0.0015 | 27.640 | 0.090 | 0.033 |
| 17 | | | 50 | 137.75 | YES | 0.1025 | 0.0025 | 137.800 | 0.050 | 0.018 |
| 18 | | | 90 | 247.95 | YES | 0.1015 | 0.0015 | 247.900 | 0.050 | 0.018 |
| 19 | LLG | 0.1 | 10 | 27.55 | YES | 0.1015 | 0.0015 | 27.660 | 0.110 | 0.040 |
| 20 | | | 50 | 137.75 | YES | 0.1020 | 0.0020 | 137.800 | 0.050 | 0.018 |
| 21 | | | 90 | 247.95 | YES | 0.1015 | 0.0015 | 247.800 | 0.150 | 0.054 |
| 22 | | 20 | 10 | 27.55 | YES | 0.1015 | 0.0015 | 27.590 | 0.040 | 0.015 |
| 23 | | | 50 | 137.75 | YES | 0.1020 | 0.0020 | 137.800 | 0.050 | 0.018 |
| 24 | | | 90 | 247.95 | YES | 0.1015 | 0.0015 | 247.900 | 0.050 | 0.018 |
| 25 | | 50 | 10 | 27.55 | YES | 0.1015 | 0.0015 | 27.620 | 0.070 | 0.025 |
| 26 | | | 50 | 137.75 | YES | 0.1025 | 0.0025 | 137.800 | 0.050 | 0.018 |
| 27 | | | 90 | 247.95 | YES | 0.1015 | 0.0015 | 247.900 | 0.050 | 0.018 |
| | | | | | Average | 0.1018 | 0.0018 | Average | 0.0678 | 0.0246 |

## 5.4. Comparison between negative and positive-sequence fault locations

The comparison of fault location errors between algorithm using negative-sequence values and algorithm using positive-sequence values is shown in Table 2. Three types of faults have been simulated (SLG, LL, and LLG). Each fault type was varied with three different fault resistances (0.1, 20 and 50 Ω) and various fault locations (10% until 90% of the line length with 10% step). In this case, the transmission line used is long transmission line which have high charging current. For each fault type, only the average, maximum and minimum values of errors for different fault locations and fault resistances were put in the table to summarize the comparison.

From Table 2, it can be seen that for SLG faults, the fault location algorithm which used the positive-sequence values has a higher average error (1.2 km or 0.436%) compared with the one which used the negative-sequence values (0.167 km or 0.06%). Both average and maximum errors for positive-sequence fault location are more than 1 km compared with average and maximum errors for negative-sequence fault location which both average and maximum errors are less than 1 km. However, for LL and LLG faults, positive-sequence fault location only has a very small increase in fault location error compared with the error for the negative-sequence fault location and thus the difference can be neglected. The average and maximum errors for LL and LLG faults for both fault location algorithms (positive and negative-sequences) are less than 1 km.

SLG fault using positive-sequence fault location has higher error than the negative-sequence fault location is because of the charging current. For long line as used in this paper, the total charging current which is distributed along the line is high. When SLG fault occurred, the charging current at the faulted phase will also include in the fault current and the charging current cannot be eliminated. The positive-sequence charging current is more than the negative-sequence charging current thus it will produce an additional effect to the fault location algorithm for SLG fault type. This is not the case for LL and LLG fault types where most of the charging current between different faulted phases will cancel each other thus will only produce a very small effect on fault location estimation.

Table 2. Comparison of errors between negative and positive-sequence fault locations

| Fault Type | km/% | Negative-Sequence Fault Location | | | Positive-Sequence Fault Location | | |
|---|---|---|---|---|---|---|---|
| | | Average | Minimum | Maximum | Average | Minimum | Maximum |
| SLG | Km | 0.167 km | 0.01 km | 0.6 km | 1.2 km | 0.05 km | 2.18 km |
| | % | 0.06% | 0.004% | 0.218% | 0.436% | 0.018% | 0.791% |
| LL | Km | 0.107 km | 0 km | 0.2 km | 0.408 km | 0.05 km | 0.68 km |
| | % | 0.039% | 0% | 0.073% | 0.148% | 0.018% | 0.247% |
| LLG | km | 0.104 km | 0.04 km | 0.2 km | 0.354 km | 0.05 km | 0.85 km |
| | % | 0.038% | 0.015% | 0.073% | 0.128% | 0.018% | 0.309% |

## 5.5. Three-phase fault location using negative-sequence values

Theoretically, negative-sequence values will not exist in a symmetrical three-phase fault condition [25]. However, a three-phase fault is very rare to happen in practice. Thus, a three-phase fault which has the same fault resistance value between phases is impossible to occur. At least there must be a slight difference of fault resistance value between phases. This will make the three-phase fault condition asymmetry so the negative-sequence fault location can be used to estimate the fault location. Two types of three-phase fault which are LLL and LLLG have been used to test the fault location algorithm. The fault resistance values for both fault types and the performance of the negative-sequence fault location in estimating the fault locations are shown in Table 3. As can be seen from the table, the errors produced for both faults are very small although negative-sequence values were used in fault location algorithm. This was due to the differences of fault resistance values between phases and phases to ground which made the faults asymmetry.

Table 3. Fault location errors for three-phase fault

| Fault Types | $R_F$ ($\Omega$) | Actual Fault Location (km) | Estimated Fault Location (km) | Error (km) | Error (%) |
|---|---|---|---|---|---|
| LLL | $R_{F, RY}$=25, $R_{F, YB}$=30 | 35 | 35.11 | 0.110 | 0.040 |
| LLLG | $R_{F, R}$=22, $R_{F, Y}$=25, $R_{F, B}$=27, $R_{F, G}$=15 | 234.175 | 234.4 | 0.225 | 0.082 |

## 6.   CONCLUSION

This paper presented the development of fault detection and location methods using sequence values and impedance-based method. Fault was detected by comparing the positive-sequence total fault current between fault condition and previous one cycle or pre-fault value. The fault location algorithm was developed using two-terminal impedance-based equation and the inputs to this algorithm are the negative-sequence values. Various faults with different fault types, fault locations and fault resistances have been successfully detected. The errors for all unsymmetrical faults are less than 1 km and 1%. The final fault location for each fault was taken at two cycles after fault detection time with the aim to avoid the unstable value of estimated fault location during transient period. To improve the accuracy of fault location, negative-sequence values have been used instead of positive-sequence values. Based on the obtained results, fault location algorithm which used negative-sequence values have better accuracy compared with the algorithm which used the positive-sequence values especially for SLG fault type. It is possible due to the negative-sequence values are not affected by the line charging current which is significant for long lines. Although negative-sequence values been chosen, the fault location algorithm also can be used to locate the three-phase faults which have different fault resistances between phases or between phases and ground. The fault resistances imbalance made the three-phase faults asymmetry which then made the negative-sequence values existed.

## REFERENCES

[1]   S. Babu, E. Shayesteh, and P. Hilber, "Analysing correlated events in power system using fault statistics," in *2016 International Conference on Probabilistic Methods Applied to Power Systems (PMAPS)*, Oct. 2016, pp. 1–6, doi: 10.1109/PMAPS.2016.7764207.

[2]   S. H. Asman, N. F. Ab Aziz, M. Z. A. Abd Kadir, and U. A. U. Amirulddin, "Fault signature analysis based on digital fault recorder in malaysia overhead line system," in *2020 IEEE International Conference on Power and Energy (PECon)*, Dec. 2020, pp. 188–193, doi: 10.1109/PECon48942.2020.9314417.

[3]    "IEEE Guide for Determining Fault Location on AC Transmission and Distribution Lines," in *IEEE Std C37.114-2014 (Revision of IEEE Std C37.114-2004)*, pp. 1-76, Jan. 2015, doi: 10.1109/IEEESTD.2015.7024095.

[4]    K. Zimmerman and D. Costello, "Impedance-based fault location experience," in *58ᵗʰ Annual Conference for Protective Relay Engineers*, 2005, vol. 2005, pp. 211–226, doi: 10.1109/CPRE.2005.1430435.

[5]    M. M. Saha, J. Izykowski, and E. Rosolowski, *Fault location on power networks*, vol. 48. London: Springer London, 2010.

[6]    C.-S. Yu, L.-R. Chang, and J.-R. Cho, "New fault impedance computations for unsynchronized two-terminal fault-location computations," *IEEE Transactions on Power Delivery*, vol. 26, no. 4, pp. 2879–2881, Oct. 2011, doi: 10.1109/TPWRD.2011.2159548.

[7]    M. B. Hessine, S. Marrouchi, and S. Chebbi, "An accurate fault location algorithm for transmission lines with use of two-end unsynchronized measurements," in *2015 IEEE 15ᵗʰ International Conference on Environment and Electrical Engineering (EEEIC)*, Jun. 2015, vol. 9, no. 2, pp. 1345–1350, doi: 10.1109/EEEIC.2015.7165365.

[8]    J. Izykowski, E. Rosolowski, P. Balcerek, M. Fulczyk, and M. M. Saha, "Accurate noniterative fault-location algorithm utilizing two-end unsynchronized measurements," *IEEE Transactions on Power Delivery*, vol. 26, no. 2, pp. 547–555, Apr. 2011, doi: 10.1109/TPWRD.2009.2031440.

[9]    F. V. Lopes, B. F. Küsel, K. M. Silva, D. Fernandes, and W. L. A. Neves, "Fault location on transmission lines little longer than half-wavelength," *Electric Power Systems Research*, vol. 114, pp. 101–109, Sep. 2014, doi: 10.1016/j.epsr.2014.04.014.

[10]   F. V. Lopes and E. J. S. Leite, "Traveling wave-based solutions for transmission line two-terminal data time synchronization," *IEEE Transactions on Power Delivery*, vol. 33, no. 6, pp. 3240–3241, Dec. 2018, doi: 10.1109/TPWRD.2018.2831458.

[11]   O. Naidu and A. K. Pradhan, "A traveling wave-based fault location method using unsynchronized current measurements," *IEEE Transactions on Power Delivery*, vol. 34, no. 2, pp. 505–513, Apr. 2019, doi: 10.1109/TPWRD.2018.2875598.

[12]   K. Andanapalli and B. R. K. Varma, "Travelling wave based fault location for teed circuits using unsynchronised measurements," in *2013 International Conference on Power, Energy and Control (ICPEC)*, Feb. 2013, pp. 227–232, doi: 10.1109/ICPEC.2013.6527656.

[13]   A. Capar and A. B. Arsoy, "ANN fault location algorithms with high speed training," in *2017 10ᵗʰ International Conference on Electrical and Electronics Engineering, ELECO 2017*, 2018, vol. 2018-January, pp. 1360–1363.

[14]   A. J. Mazon, I. Zamora, J. F. Miñambres, M. A. Zorrozua, J. J. Barandiaran, and K. Sagastabeitia, "A new approach to fault location in two-terminal transmission lines using artificial neural networks," *Electric Power Systems Research*, vol. 56, no. 3, pp. 261–266, Dec. 2000, doi: 10.1016/S0378-7796(00)00122-X.

[15]   D. C. Huynh, T. H. Truong, and M. W. Dunnigan, "Optimization-based fault location on double-circuit transmission lines of power system," in *2021 5ᵗʰ International Conference on Electrical, Electronics, Communication, Computer Technologies and Optimization Techniques (ICEECCOT)*, Dec. 2021, pp. 746–751, doi: 10.1109/ICEECCOT52851.2021.9707918.

[16]   Y. Liu, A. P. S. Meliopoulos, Z. Tan, L. Sun, and R. Fan, "Dynamic state estimation-based fault locating on transmission lines," *IET Generation, Transmission and Distribution*, vol. 11, no. 17, pp. 4184–4192, Nov. 2017, doi: 10.1049/iet-gtd.2017.0371.

[17]   Y. Liu, B. Wang, X. Zheng, D. Lu, M. Fu, and N. Tai, "Fault location algorithm for non-homogeneous transmission lines considering line asymmetry," *IEEE Transactions on Power Delivery*, vol. 35, no. 5, pp. 2425–2437, Oct. 2020, doi: 10.1109/TPWRD.2020.2968191.

[18]   S. F. Mekhamer, A. Y. Abdelaziz, M. Ezzat, and T. S. Abdel-Salam, "Fault location in long transmission lines using synchronized phasor measurements from both ends," *Electric Power Components and Systems*, vol. 40, no. 7, pp. 759–776, Apr. 2012, doi: 10.1080/15325008.2012.658599.

[19]   M. Davoudi, J. Sadeh, and E. Kamyab, "Parameter-free fault location for transmission lines based on optimisation," *IET Generation, Transmission and Distribution*, vol. 9, no. 11, pp. 1061–1068, Aug. 2015, doi: 10.1049/iet-gtd.2014.0425.

[20]   K. Kalita, S. Anand, and S. K. Parida, "A novel non-iterative fault location algorithm for transmission line with unsynchronized terminal," *IEEE Transactions on Power Delivery*, vol. 36, no. 3, pp. 1917–1920, Jun. 2021, doi: 10.1109/TPWRD.2021.3054235.

[21]   Schweitzer Engineering Laboratories, "SEL-T401L ultra high speed line relay intruction manual," SEL-T401L Data Sheet, 2021, Accessed: Jul. 05, 2021. [Online]. Available: https://docplayer.net/194979821-Sel-t401l-ultra-high-speed-line-relay.html

[22]   Y. Xue, D. Finney, and B. Le, "Charging current in long lines and high-voltage cables – protection application considerations," in *39th Annual Western Protective Relay Conference*, 2013, pp. 1–18.

[23]   S. Roostaee, M. S. Thomas, and S. Mehfuz, "Experimental studies on impedance based fault location for long transmission lines," *Protection and Control of Modern Power Systems*, vol. 2, no. 1, Dec. 2017, doi: 10.1186/s41601-017-0048-y.

[24]   L. Lima, "IEEE PES Task Force on Benchmark Systems for Stability Controls," Report on the 14-generator system (Australian Reduced Model), 2013.

[25]   A. Amberg and A. Rangel, "Tutorial on symmetrical components," *Selinc.Cachefly.Net*, no. 1. pp. 1–6, 2014.

## BIOGRAPHIES OF AUTHORS

**Muhd Hafizi Idris** 🆔 📗 SC ⬡ received the Bachelor of Engineering degree in Electrical and Electronic from Universiti Kebangsaan Malaysia (UKM) in 2006, Master of Engineering in Electrical (Power) from Universiti Teknologi Malaysia (UTM) in 2011 and PhD degree from Universiti Malaysia Perlis (UniMAP) in 2022. From 2006 until 2009, he worked as protection engineer with Tenaga Nasional Berhad (TNB). Currently, he is a lecturer and researcher at Faculty of Electrical Engineering and Technology, Universiti Malaysia Perlis (UniMap). His fields of interest including power system protection, fault location, artificial intelligence (AI) and Internet of thing (IoT) application. He can be contacted at email: hafiziidris@unimap.edu.my.

**Mohd Rafi Adzman** 🆔 �颐 ⑤ᴄ ○ received the M.Sc. degree in power system and high voltage Engineering from Helsinki University of Technology, Finland, in 2006, and the D.Sc. degree in Technology from Aalto University, Finland, in 2014. In 2001, he was a Project Engineer with Foxboro, Malaysia. Then, he joined Power Cable Malaysia, as an Electronic Engineer in 2003. He has been with the Faculty of Electrical Engineering & Technology, Universiti Malaysia Perlis (UniMAP) since 2004. His current research interests include renewable energy, power system distribution automation, fault localization, power quality and artificial intelligent application in power systems. He is a member of the International Association of Engineers (IAENG) and the Board of Engineers Malaysia (BEM), Malaysia. He can be contacted at email: mohdrafi@unimap.edu.my.

**Hazlie Mokhlis** 🆔 🔻 ⑤ᴄ ○ received the B. Eng. and M. Eng. Sc. degrees in Electrical Engineering from the University of Malaya (UM), Malaysia, in 1999 and 2002, respectively and the Ph.D. degree from The University of Manchester, Manchester, U.K., in 2009. He is currently a Professor with the Department of Electrical Engineering, UM, and the Head of the UM Power and Energy System (UMPES). His research interests include fault location, distribution automation, power system protection, and renewable energy. He is also a Chartered Engineer in U.K., and a Professional Engineer in Malaysia. He can be contacted at: hazli@um.ed.my.

**Lilik Jamilatul Awalin** 🆔 🔻 ⑤ᴄ ○ received the B. Eng. degree in Electrical Engineering in 1999 from the University of Widya Gama, M. Eng. degree in 2004 from the Institut Teknologi Sepuluh Nopember, Indonesia and Ph.D. degree in 2014 from University of Malaya. She was a Senior Lecturer in 2015 until 2020 in University Kuala Lumpur, Electrical Engineering Section, British Malaysia Institute, Gombak, Selangor, Malaysia. Currently, she is a senior lecturer in Airlangga University, Indonesia. Her research interest includes fault location, protection system, distribution and transmission system and smart grid. She can be contacted at: lilik.j.a@ftmm.unair.ac.id.

**Mohammad Faridun Naim Tajuddin** 🆔 🔻 ⑤ᴄ ○ received the B. Eng. and M. Eng. degrees from the University of Malaya (UM), Malaysia, in 2004 and 2007, respectively and the Ph.D. degree from the Universiti Teknologi Malaysia (UTM), Johor, Malaysia, in 2015. He is currently an Associate Professor with the Faculty of Electrical Engineering and Technology, Universiti Malaysia Perlis (UniMAP). He has published refereed manuscripts in various reputable international journals. His research interests include power electronics control, photovoltaic modeling and control, intelligent control, and optimization techniques. He also acts as a Reviewer for various reputed journals, such as the IEEE, Applied Energy (Elsevier), Renewable and Sustainable Energy Reviews, Neurocomputing and Energy Reports. He can be contacted at email: faridun@unimap.edu.my.